Materials Research. 2014; 17(2): 303-310
DOI: http://dx.doi.org/10.1590/S1516-14392014005000039

Ab. Initio Study of the Structural, Elastic, Electronic and Optical Properties of Cu_3N

A. Rahmati[a,b,c], M. Ghoohestani[d], H. Badehian[e], M. Baizaee[a]*

[a]*Department of Physics, Faculty of Science, Vali-e-Asr University of Rafsanjan, Rafsanjan, Iran*
[b]*Nano Research Group, Vali-e-Asr University of Rafsanjan, Rafsanjan, Iran*
[c]*Thin Film Laboratory, Faculty of Science, Vali-e-Asr University of Rafsanjan, Rafsanjan, Iran*
[d]*Nano Research Centre, Department of Physics, Malek Astar University of Technology, Shahinshahr, Isfahan, Iran*
[e]*Condensed Matter Lab, Department of Physics, Faculty of Science, Shahid Chamran University, Ahvaz, Iran*

Received: February 20, 2013; Revised: January 14, 2014

Electronic, optical, elastic, properties of Copper nitride (Cu_3N) in cubic anti- ReO_3 phase have been studied using the full-potential augmented plane waves (FP-LAPW) within density functional theory (DFT) framework. Generalized gradient approximation (GGA), local density approximation (LDA), Perdew– Burke–Ernzerhof generalized parameterization of gradient approximation (GGA-PBE), and new modified Becke and Johnson GGA (MBJ-GGA) have been used for exchange-correlation potentials. The structural properties such as equilibrium lattice parameter, bulk modulus and its pressure derivative have been obtained and optimized. The Hubbard potential has been enhanced to improve bandgap energy. Optical properties, such as the dielectric function, refractive index, extinction index, and optical band gap, were calculated for radiation up to 14 eV. The chemical bonding in Cu_3N was discussed by three method electronegativity concept, B/G ratio, and charge density distribution. Moreover, Elastic constants, Young's modulus, shear modulus, Poisson's ratio, sound velocities for longitudinal and shear waves, Debye average velocity and Debye temperature have been calculated. The estimated structural, elastic and other parameters are in good agreement with experimental data. The calculation exhibits that Cu_3N is a direct semiconductor (0.7-1.12 eV) with ductile and ionic identity.

Keywords: *band structure, density of states, elastic constants, Debye temperature*
The PACS: 71.20.Be, 71.20.Gj, 81.05.Bx describe the paper well

1. Introduction

Many interests were concentrated on copper nitride for several reasons; copper nitride can be used as an optical engraving medium for optoelectronic devices[1], a barrier material in spin tunnel junction[2], a high density optical storage media[3,4], micrometric conductive dots and lines[5] and good candidate for hybrid inorganic solar cells[6].

Copper nitride has several phases among which cubic anti-ReO_3 structure is more stable. In this phase Copper nitride has simple cubic structure and is crystallized in space group pm-3 m (221) with atomic positions Cu (0, 0, 0) and N (1/2, 1/2, 1/2). Unit cell of Cu3N is illustrated in Figure 1.

There are always noticeable divergences between values of theoretically calculated band gap energy and experimental ones. According to the theoretical works, Cu_3N is semiconductor with narrow band gap in 0.23 to 0.9 eV regions[7,8] whereas, experimental results change between 0.8 to 1.9 eV[6,9-11].

In this study, we have studied structural, elastic, optical, and electronic properties of yttrium oxide compound in cubic phase using the full-potential augmented plane waves (FP-LAPW) within density functional theory (DFT) framework. Moreover, we have used new approximation for exchange and correlation terms (MBJ-GGA) for band calculation which greatly improves the band gap. Our results agree very well with experimental studies. Some experimental results were incorporated to validate theoretical results.

*e-mail: a.rahmati@vru.ac.ir

2. Computational Method

The full-potential linear augmented plane wave (FP-LAPW) method implemented in WIEN2K (2011) computer package[12]. In this method the space is divided into an interstitial region (IR) and non-overlapping (MT) spheres centered at the atomic sites. the basis set consists of plane waves, in the IR region. In the MT spheres, the basis sets is described by radial solutions of the one particle Schrodinger equation (at fixed energy) and their energy derivatives multiplied by spherical harmonics. To achieve energy eigenvalues convergence, the wave functions in the interstitial region were expanded in plane waves with a cut-off, $K_{max} = 14/R_{mt}$ where R_{mt} denotes the smallest atomic sphere radius and K_{max} gives the magnitude of the largest K vector in the plane wave expansion. For Cu_3N, the radius values R_{mt} are taken to be 1.7 and 1.5 atomic units (a.u.) for Cu and N respectively. The full-potential methods the calculation is dependent on the choice of sphere radii in the full-potential methods. The valence wave functions inside the spheres are expanded up to $l_{max} = 10$, while the charge

density was Fourier expanded up to G_{max} = 14 $(a.u.)^{-1}$. The exchange– correlation (XC) effect was treated by the generalized gradient approximation (GGA), GGA+U, mBJ and mBj+U. The self-consistent calculations are considered to be converged when the total energy of the system is stable within 10^{-4} Ry. The integrals over the irreducible Brillouin zone (IBZ) are performed up to 35 k-points, using the Monkhorst–Pack special k-points approach[13]. To validate the results, the calculated reflectance spectra, refractive index and absorption coefficient were compared with their corresponding experimental results.

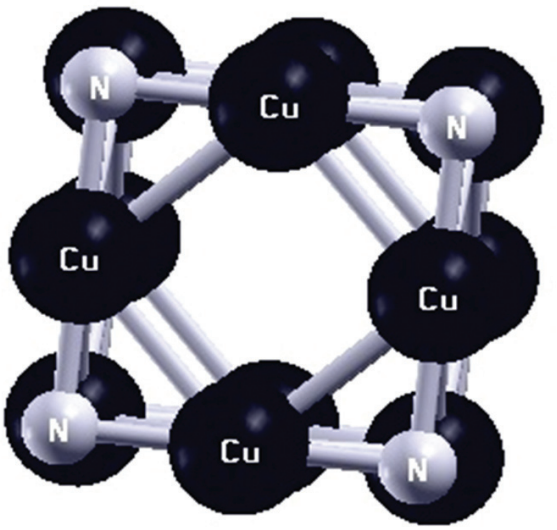

Figure 1. Unit cell of Cu_3N.

3. Results and Discussions

3.1. *Structural properties*

Figure 2 shows the calculated total energy of Cu_3N structure by GGA, LDA and GGA+SP approaches. To obtain the ground state properties, the total energies are fitted to Murnaghan[14] equation of state

$$E(V) = E_0 + \frac{B_0 V_0}{B'}\left[\frac{V}{V_0} + \frac{(V/V_0)^{1-B'} - B'}{B'-1}\right] \quad (1)$$

where P is the pressure, V is the volume at pressure P, V_0 is the volume at ambient pressure, B_0 is the bulk modulus at ambient pressure and B' is the pressure derivative of bulk modulus B_0.

The equilibrium lattice constant, bulk modulus and pressure derivative of the bulk modulus are given in Table 1, together with some theoretical results and the available experimental data. It is clearly seen that the LDA

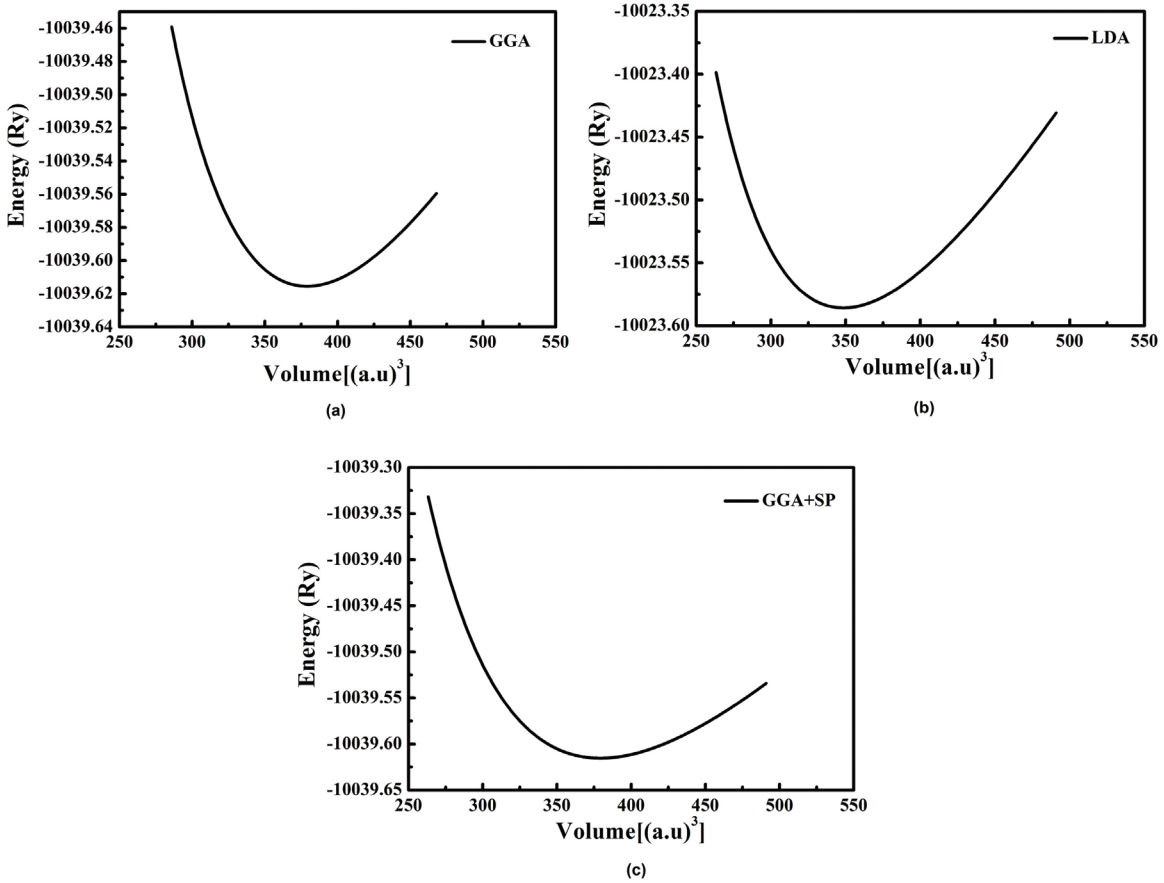

Figure 2. Total energy versus the atomic volume for cubic Cu_3N. by (a) GGA, (b) LDA and (c) GGA+SP approximations.

under-estimates (over-estimates) the lattice parameters (Bulk modulus) while the GGA and GGA+SP results are in reasonable agreement with the experimental and other calculated values.

3.2. *Electronic properties*

In order to investigate electronic properties, the band structure and density of states (DOS) were calculated. Figure 3 depicts the calculated band structure and total DOS for Cu_3N by GGA. There are three regions. First; a sharp peak under -15 eV (related to Nitrogen 2s orbitals), second; wide valance band about 8 eV, third; conduction band. From partial DOS (Figure 4), there is strong hybridization between N and Cu states mostly related to N 2p and Cu 3d orbitals. Moreover, it is understood that Cu_3N compound is a semiconductor with indirect band gap. The maximum valance band is at R point and the minimum conduction band is at M point.

There are noticeable differences between values of theoretically calculated band gap energy and experimental ones. According to the theoretical works, Cu_3N is semiconductor with narrow band gap in 0.23 to 0.9 eV regions[6,7] whereas, experimental results change between 0.8 to 1.9 eV[6,9-11]. The calculated bandgap energy by different approaches was listed in Table 2. By applying GGA-PBE (PBE0) and MBJ-GGA approaches, the direct band gap were estimated to be 0.85 and 1.04 eV that improved in comparison to GGA and predicted in the range of experimental results.

To coincide the calculated bandgap energy with the experimental one, the Hubbard parameter U was introduced to guarantee spatial distribution of the partially filled d orbitals[15]. The U values were calculated to be 5.2eV for Cu_3N using Wien2K package. By applying GGA+U and MBJ+U approaches, the band gap was calculated 0.95 and 1.12 eV, respectively. This confirms the latter approach was suitable to calculate band gap in semiconductors as reported by Tran et al.[16]. Using MBJ, the band gap was obtained 1.04 eV that improve our previous results and other's results. Then effective potential (U) was added to MBJ and the band gap is calculated 1.12 eV (see Table 2). In Figure 4, the band structure, the total and atomic densities of states of Cu_3N by GGA+U and MBJ+U are depicted to analogy with other approaches.

Table 1. The equilibrium lattice constant *a* (Å), bulk modulus B_0 (GPa), pressure derivative of bulk modulus *B' calculated using GGA, LDA, GGA+SP approximation*.

Structural properties / *Approximation*	*a* (Å)	B_0 (GPa)	*B'*
GGA	3.829	113.9	4.50
LDA	3.72	145.98	4.87
GGA+SP	3.829	113.9	4.50
Other results	3.82-3.85[1-9]	104-114[7,9,12]	4.66-5.26[7,12]

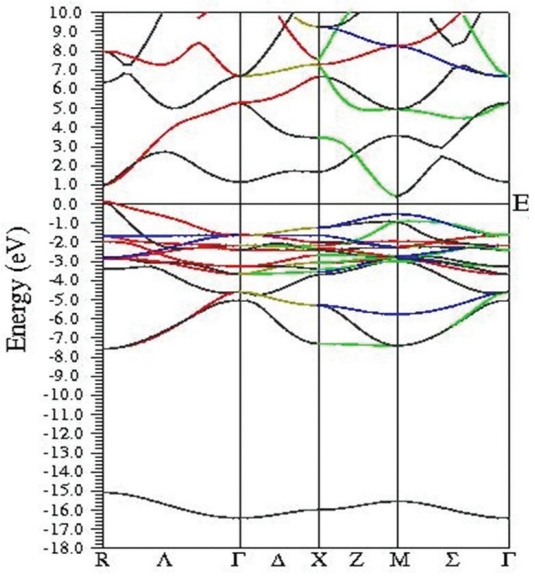

Figure 3. Band structure of Cu3N at the ground state by using GGA approximation.

3.3. *Optical properties*

The optical properties of matter can be described by the complex dielectric function ε(ω), which represents the linear response of a system to an external electromagnetic field. It can be expressed as $\varepsilon(\omega) = \varepsilon_1(\omega) + i\varepsilon_2(\omega)$, where $\varepsilon_1(\omega)$ and $\varepsilon_2(\omega)$ are the real and imaginary parts of the dielectric function, respectively. Generally, there are two contributions to ε(ω), namely, intra-band and inter-band transitions. The contribution from intraband transitions is crucial only for metals. The interband transitions can further be split into direct and indirect transitions. The indirect inter-band transitions which involved scattering of phonon was ignored. The imaginary part $\varepsilon_2(\omega)$ is directly related to the electronic band structure and it can be computed by summing up all possible transitions from the occupied to the unoccupied states, taking into account the appropriate transition dipole matrix elements. A full detail description of the calculation of these matrix elements is given by Ambrosch-Draxl et al.[17]. The real part $\varepsilon_1(\omega)$ can be derived from the imaginary part using the familiar Kramers–Kronig transformation. The knowledge of both real and imaginary parts of the dielectric function allows the calculation of various optical constants, such as the spectral reflectivity, the refractive index, and the electron energy loss function using standard expressions[18].

Absorption coefficient is given according to Tauc-Pankove relation[19]

$$\alpha E = B(E - E_g)^p \quad (2)$$

where *E* is the photon energy, and *B* is a factor depends on the transition probability and can be assumed to be constant within the optical frequency range, and the index *p* is related to the distribution of the density of states. The index *p* has discrete values like 1/2, 3/2, 2, more depending on whether the transition is direct or indirect and allowed or forbidden.

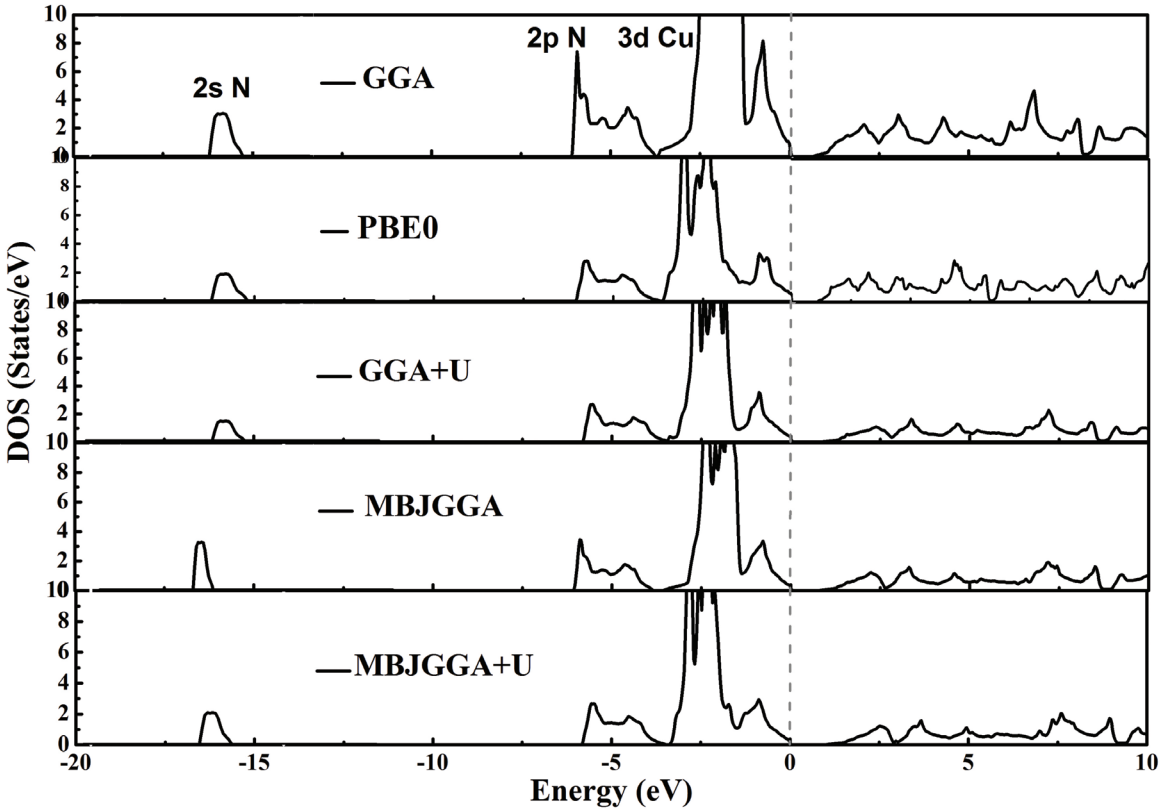

Figure 4. Total and partial density of states of Cu_3N at the ground state by using GGA, PBE0, GGA+U, MBJ and MBJ+U approximations.

Table 2. The calculated bandgap energy and comparison with other results.

Other results		MBJ+U	MBJ	GGA+U	PBE0	GGA	
Experimental[6,9,13]	Theoretical[1,7,8]						
0.8-1.9	0.23-0.9	1.12	1.04	0.95	0.85	0.7	Bandgap energy (eV)

The optical energy gap was deduced from the intercept of the extrapolated liner part of the plot of $(\alpha E)^{1/p}$ versus the photon energy E with abscissa. The band energy Cu_3N is calculated according to $(\alpha E)^{1/p}$- E using Figure 5ain the frame of GGA, GGA+U and MBJ approaches. the optical band gap from these approaches were estimated 0.9, 1.3 and 1.5 eV, respectively.

The refractive index dispersion was calculated using GGA, GGA+U and MBJ approaches (Figure 5b). The phonon contributions are not included to the dielectric screening. $\varepsilon_1(\omega)$ corresponds to the static optical dielectric constant. The static refractive index was 3.3, 2.9 and 2.7 for GGA, GGA+U and MBJ, respectively.

Transmittance and reflectance spectra were measured for as-deposited Cu_3N thin films by reactive magnetron sputtering at different substrate temperature[9]. Figure 6a depicts the plot of Tauc- pankove relation versus photon energy. It is seen the theoretical and experimental bandgap energy are in good agreement. Figure 6b illustrates the refractive index dispersion of the Cu_3N thin films. Cauchy dispersion relation[20]

$$n(\lambda) = n_0 + n_1E^2 + n_2E^4 \quad (3)$$

was fitted with refractive index extracted from experimental transmittance and reflectance data and the n_0, static refractive index, was obtained as 2.66-3.04 for Cu_3N thin films (see the corresponding theoretical value).

3.4. *Electronic charge distribution*

Figure 7 depicts the electronic charge distribution in (110) plane of Cu_3N structure. The electon cloud distribution slightly deformed between neighbors Cu- N bond. To confirm the iconicity of the bound, according to Hanney-Smyth relation[21], the iconicity of A- B bond is

$$ti\ (\mathrm{HS}) = 0.16 \mid \chi_A - \chi_B \mid + 0.35 \mid \chi_A - \chi_B \mid^2 \quad (4)$$

where χ_A and χ_B is the electronegativity of the involving atoms. χ_{Cu} = 1.90 and χ_N = 3.04. The iconicity of the chemical Cu- N bound is around 0.63. Hence, Cu_3N is mostly ionic. It confirms small deformation in electronic distribution between Cu- N bound.

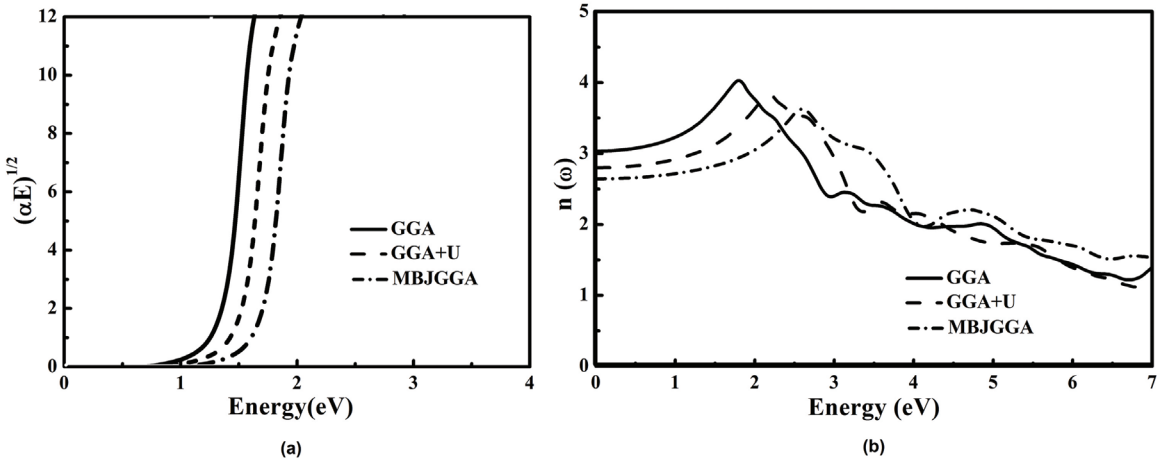

Figure 5. (a) The $(\alpha E)^{1/2}$-E to calculate the band gap energy (b) the refractive coefficient of Cu_3N.

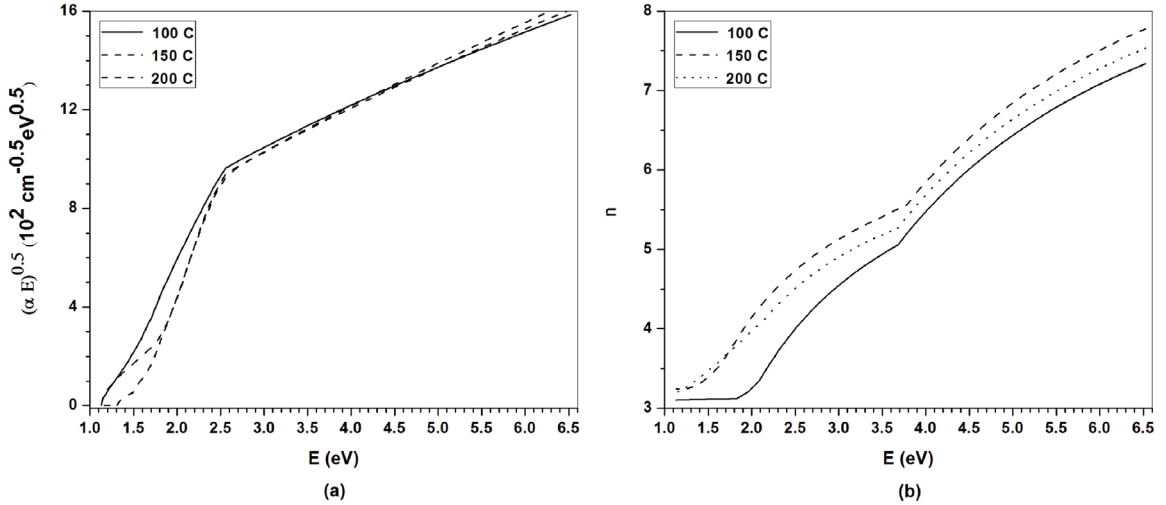

Figure 6. The plot of Tauc- Pankove relation (a) and dispersion of refractive index (b). (The related data are extracted from measured absorption coefficient, transmittance and reflectance).

3.5. *Elastic constants and mechanical properties*

The elastic constants C_{ij} are the proportionality coefficients relating the applied strain (ε_i) to the stress (σ_i), $\sigma_i = C_{ij}\varepsilon_i$. So, C_{ij} determines the response of the crystal to external forces[22]. Ab initio calculation of the elastic constants is based on induced changes in the total energy due to the changes in the strain[23-25].

The symmetry of cubic crystal lattice reduces the 21 elastic constants to three independent elastic constants namely C_{11}, C_{12} and C_{44}[26]. The present values of elastic constants of Cu_3N using GGA were given in Table 3. The elastic stability criteria for a cubic crystal[27] at ambient condition (P=1bar and room temperature) are simultaneously $C_{11}+2C_{12}>0$, $C_{44}>0$ and $C_{11}-C_{12}>0$. The elastic constants were calculated using the tetrahedral and rhombohedral distortions on the cubic structure. The systems are fully relaxed after each distortion in order to reach the equilibrium state[28]. This optimization procedure was important for rhombohedral case, in which the accurate results could be obtained for C_{44}. The elastic anisotropy ratio is another important physical quantity which tells about the structural stability and it is highly correlated with the possibility of inducing micro-cracks in the materials. This is defined as $A=2C_{44}/(C_{11}-C_{12})$. For a completely isotropic system, A is unity and the deviation from unity measures the degree of elastic anisotropy[28]. This factor was also calculated. The anisotropy factor values of Cu_3N do not deviate much from the unity, hence Cu_3N was not described by a profound anisotropy.

Voigt-Reuss[29-30] approach, the actual effective modulus for crystals could be approximated by the arithmetic mean of the two well-known bounds for mono crystals. Then the main mechanical parameters for cubic structures, i.e. shear modulus G, bulk modulus B, Young's modulus E, Poisson's ratio σ and Lame's coefficients μ and λ were calculated from the elastic constants of the single crystals using the following relations:

$$G = (C_{11} - C_{12} + 3C_{44})/5 \quad (5a)$$

Table 3. The elastic constants of Cu_3N.

Elastic constants	C_{11}(GPa)	C_{12}(GPa)	C_{44}(GPa)	B(GPa)	E(GPa)	A	σ	μ (GPa)	λ (GPa)	G(GPa)	B/G
Peresent work	249.910	49.557	35.090	116.342	156.045	0.35	0.28	60.94	77.58	61.125	1.9
Others results [22]	234.2	54.4	17.5	114.3	122.8	-	-	-		46.5	2.4

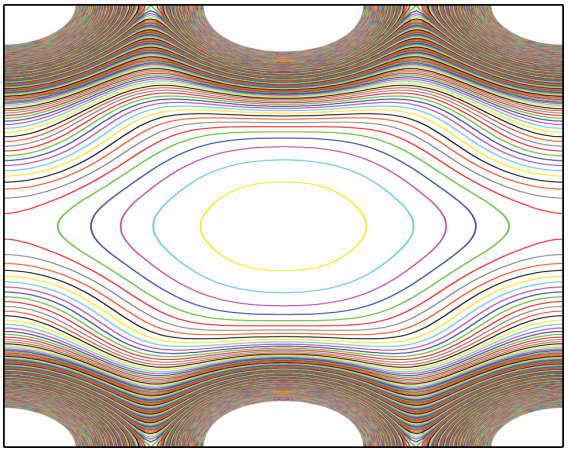

Figure 7. Electron density maps of Cu_3N in the (110) plane.

$$B=\frac{1}{3}(C_{11}-2C_{12}) \quad (5b)$$

$$E = 9BG/(3B + G) \quad (5c)$$

$$\sigma = (3B-E)/(6B) \quad (5d)$$

$$\mu = E/2(1 + \sigma) \quad (5e)$$

$$\lambda = \sigma E/\{(1 + \sigma)(1 - 2\sigma)\} \quad (5f)$$

The value of the Poisson ratio σ for covalent materials is small as σ = 0.1, whereas for ionic materials a typical value of σ is 0.25[31]. The value of σ was calculated to be about 0.28, i.e. a ionic contribution in intra-atomic bonding for Cu_3N was confirmed (see section 3.4).

The bulk modulus B as calculated from elastic constant (116.342GPa) is in good agreement with the corresponding data in Table 1. According to the empirical Pugh formula[32], the critical value of the ratio B/G separates the ductile and brittle behavior of materials is around 1.75; i.e. if B/G > 1.75, the material behaves in a ductile manner; otherwise the material behaves in a brittle manner. Therefore, Cu_3N was classified as brittle material.

Using the Young's modulus E, bulk modulus B, and shear modulus G, mean velocity (v_m) and Debye temperature (θ_D) could been calculated. θ_D is an important fundamental parameter closely related to many physical properties such as elastic constants, specific heat and melting temperature. θ_D can be estimated from the elastic constants data, by the following classical relations[33]:

$$\theta_D=\frac{h}{k_B}\left[\frac{3}{4\pi V_a}\right]^{1/3} v_m \quad (6)$$

Table 4. The calculated density (ρ, in g/cm^3), longitudinal, transverse and average sound velocity (v_l, v_t and v_m, in m/s) and Debye temperature (θ_D, in K) for Cu_3N.

Compound	ρ	v_t	v_l	v_m	θ_D
Cu_3N	3.64	4097.9	7372.4	4563.9	353

where v_m is the mean sound velocity, h is Plank's constant, k_B is Boltzmann's constant and V_a is the atomic volume. The mean sound velocity in the polycrystalline material is given by[34]:

$$v_m=\left[\frac{1}{3}\left(\frac{2}{v_t^3}+\frac{1}{v_l^3}\right)\right]^{-1/3} \quad (7)$$

where v_l and v_t are the longitudinal and transverse elastic wave velocities, respectively, in an isotropic material, which can be obtained using the shear modulus G and the bulk modulus B from Navier's equation[35]:

$$v_l=\left[\frac{3B+4G}{3\rho}\right]^{1/2} \text{ and } v_t=\left(\frac{G}{\rho}\right)^{1/2} \quad (8)$$

The calculated sound velocity and Debye temperature as well as the density for Cu_3N are given in Table 4. Unfortunately, as far as the authors know, there are no data available related to these properties in the literature for this compound. Future experimental work will testify the calculated results.

3.6. *The cohesive energy*

First principles calculations based on the DFT is a useful tool to determine the cohesive energy of the solids. The cohesive energy is defined as the difference between the energy of an isolated atom and the energy of the same atom in the solid. In order to calculate cohesive energy, the energy of an isolated atom by considering it to be in a large unit cell containing just one atom, with FCC crystal structure irrespective of crystal structure of the corresponding solid. This does not introduce any errors in the results, due to the fact that a very large unit cell has been considered in the calculations. The size of the unit cell was chosen sufficiently large so that the energy convergence with respect to the size of the cell was less than 0.0001 Ry: a large cubic cell with dimensions of 25 a.u. was used for Cu and N. The energy of isolated Cu and N atoms are E_{tot} (Cu)= -3309.77129537 Ry and E_{tot} (N)= -108.91055867 Ry, respectively. The energy of the same atom in the solid as Cu_3N is $E_{tot}(Cu_3N)$= -10039.61508342Ry.The cohesive energy of Cu_3N is calculated as $\Delta E(Cu_3N)=E_{tot}^{Cu_3N}-(3E_{tot}^{Cu}-E_{tot}^{N})=-1.39Ry$

4. Conclusion

In summary, ab-initio calculations of structural, electronic, optical and elastic properties of Cu_3N using full-potential linearized augmented plane-wave method. The calculations were done using different approaches for exchange-correlation term including GGA, LDA, PBE, and as well as new approximation MBJ-GGA. The addition of Hubbard potential parameter improved the predicted bandgap energy. The optimized structural parameters were in good agreement with the experimental ones. The elastic constants and derived bulk modulus, shear modulus, Young's modulus, Poisson's ratio, and sound velocities for longitudinal and shear waves were calculated.

The calculated elastic constants satisfied the stability criteria. The Debye temperature was calculated. The results showed that Cu_3N is brittle. Moreover, the results of electronegativity concept, electronic charge density and Poisson's ratio revealed that the bonding nature between Cu–N was governed by ionic identity. The direct band gap energy (about 1.12 eV) which obtained by MBJ+U, are well in agreement with experimental result. The static refractive index was 2.7-3.3 that extracted from dispersion of refractive index. The optical band gap energy obtained using Tauc –Ponkove relation is greater than that of predicted by band structure.

The static equilibrium lattice structure, elastic constants bulk modulus and Debye temperature of the cubic anti-ReO_3 structural copper nitride (Cu_3N) were calculated using a first-principles full-potential linearized augmented plane wave (FP-LAPW). For the exchange-correlation terms, GGA, GGA + U, PBE0, MBJ and MBJ + U approximations have been used. The bandgap energy of Cu_3N has been calculated using effective potential U estimated by ab-initio study and improved with respect to the other theoretical works. The refractive index and optical gap have been calculated and compared with other studies. Moreover, mechanical stability of Cu_3N was confirmed using the calculated mechanical and elastic constants.

References

1. Moreno-Armenta MG, Soto G and Takeuchi N. Ab initio calculations of non-stoichiometric copper nitride, pure and with palladium. *Journal of Alloys and Compounds.* 2011; 509(5):1471-1476. http://dx.doi.org/10.1016/j.jallcom.2010.09.192
2. Borsa DM, Grachev S and Boerma DO. Development of epitaxial nitride-based bilayers for magnetic tunnel junctions. *IEEE Transactions on Magnetics*. 2002; 38(5):2709-2711. http://dx.doi.org/10.1109/TMAG.2002.803156
3. Asano M, Umeda K and Tasaki A. Cu_3N Thin Film for a New Light Recording Media. *Japanese Journal of Applied Physics*. 1990; 29:1985-1986. http://dx.doi.org/10.1143/JJAP.29.1985
4. Maruyama T and Morishita T. Copper nitride and tin nitride thin films for write once optical recording media. *Applied Physics Letters*. 1996; 69:890. http://dx.doi.org/10.1063/1.117978
5. Nosaka T, Yoshitake M, Okamoto A, Ogawa S and Nakayama Y. Thermal decomposition of copper nitride thin films and dots formation by electron beam writing. *Applied Surface Science*. 2001; 169-170:358-361. http://dx.doi.org/10.1016/S0169-4332(00)00681-4
6. Navio C, Capitan M J, Alvarez J, Yndurain F and Miranda R. Intrinsic surface band bending in Cu_3N(100) ultrathin films. *Physical Review B.* 2007; 76:085105. http://dx.doi.org/10.1103/PhysRevB.76.085105
7. Armenta MGM, Martinez A and Takeuchi N. Ab initio total energy calculations of copper nitride: the effect of lattice parameters and Cu content in the electronic properties. *Solid State Sciences.* 2004; 6(1):9-14. http://dx.doi.org/10.1016/j.solidstatesciences.2003.10.014
8. Hou ZF. Effects of Cu, N, and Li intercalation on the structural stability and electronic structure of cubic Cu_3N. *Solid State Sciences*. 2008; 10(11):1651-1657. http://dx.doi.org/10.1016/j.solidstatesciences.2008.02.013
9. Hadian F, Rahmati A, Movla H and Khaksar M. Reactive DC magnetron sputter deposited copper nitride nano-crystalline thin films: Growth and characterization. *Vacuum.* 2012; 86(8):1067-1072. http://dx.doi.org/10.1016/j.vacuum.2011.09.001
10. Gonzalez-Arrabal R, Gordillo N, Martin Gonzalez MS, Ruiz Bustos R and Agullo-Lopez F. Thermal stability of copper nitride thin films: The role of nitrogen migration. *Journal of Applied Physics.* 2010; 107:103513. http://dx.doi.org/10.1063/1.3369450
11. Yu W, Li LY and Jin CQ. Pressure induced metallization of Cu_3N. *Journal of Materials Science*. 2005; 40(17):4661-4664. http://dx.doi.org/10.1007/s10853-005-0638-3
12. Blaha KSP, Madsen G, Kvasnika D and Luitz K. *WIEN2k, an Augmented Plane Wave Plus Local Orbitals Program for Calculating Crystal Properties.* Wien: Karlheinz Schwarz, Techn. Universit€at Wien; 2001.
13. Monkhorst HJ and Pack JD. Special points for Brillouin-zone integrations. *Physical Review B.* 1976; 13(12):5188-5192. http://dx.doi.org/10.1103/PhysRevB.13.5188
14. Murnaghan FD. The compressibility of media under extreme pressures. *Proceedings of the National Academy of Sciences of the United States of America*. 1944; 30(9):244. http://dx.doi.org/10.1073/pnas.30.9.244
15. Georg K, Madsen H and Novak P. *Calculation the effective U in APW methods. NiO.* 2007. Available from: <http://www.wien2k.at/reg_user/textbooks/Constraint_U.pdf>.
16. Tran F. and Blaha P. Accurate Band Gaps of Semiconductors and Insulators with a Semilocal Exchange-Correlation Potential. *Physical Review Letters.* 2009; 102:226401. http://dx.doi.org/10.1103/PhysRevLett.102.226401
17. Ambrosch-Draxl C and Sofo JO. Linear optical properties of solids within the full-potential linearized augmented planewave method. *Computer Physics Communications*. 2006; 175(1):1-14. http://dx.doi.org/10.1016/j.cpc.2006.03.005
18. Delin A, Eriksson AO, Ahuja R, Johansson B, Brooks MSS, Gasche T et al. Optical properties of the group-IVB refractory metal compounds. *Physical Review B.* 1996; 54(3):1673-1681. http://dx.doi.org/10.1103/PhysRevB.54.1673
19. Patterson J and Bailey B. *Solid-State Physics, Introduction to the theory*. 2nd ed. Springer; 2010.

20. Singh J. *Optical Properties of Condensed Matter and Applications*. John Willey & Sons Ltd.; 2006. http://dx.doi.org/10.1002/0470021942
21. Hanney NB and Smyth CP. The Dipole Moment of Hydrogen Fluoride and the Ionic Character of Bonds. *Journal of the American Chemical Society*. 1946; 68(2):171-173. http://dx.doi.org/10.1021/ja01206a003
22. Seddik T, Khenata R, Bouhemadou A, Reshak AH, Semari F and Amrani B. Prediction study of the structural, elastic and high pressure properties of Yttrium chalcogenide. *Computational Materials Science*. 2010; 49(2):372-377. http://dx.doi.org/10.1016/j.commatsci.2010.05.024
23. Mehl MJ. Pressure dependence of the elastic moduli in aluminum-rich Al-Li compounds. *Physical Review B*. 1993; 47(5):2493-2500. http://dx.doi.org/10.1103/PhysRevB.47.2493
24. Khenata R, Bouhemadou A, Reshak AH, Ahmed R, Bouhafs B, Rached D et al. First-principles calculations of the elastic, electronic, and optical properties of the filled skutterudites $CeFe_4P_{12}$ and $ThFe_4P_{12}$. *Physical Review B*. 2007; 75(19):195131. http://dx.doi.org/10.1103/PhysRevB.75.195131
25. Bouhemadou A, Khenata R, Zegrar F, Sahnoun M, Baltache H and Reshak AH. Ab initio study of structural, electronic, elastic and high pressure properties of barium chalcogenides. *Computational Materials Science*. 2006; 38(2):263-270. http://dx.doi.org/10.1016/j.commatsci.2006.03.001
26. Kittel C. *Introduction to solid state physics.* 8th ed. John Wiley & Sons Inc.; 2005.
27. Born M and Hang K. *Dynamical Theory and Experiments I*. Berlin: Springer Verlag Publishers; 1982.
28. Voight W. *Lehrbuch Der Kristallphysik*. Johnson Reprint Corp; 1928.
29. Reuss A and Angew Z. Berechnung der fliessgrenze von mischkristallen auf grund der plastizitasbendingung fur einkristalle. *Journal of Applied Mathematics and Mechanics.* 1929; 9(1):40-58.
30. Edward S, Anderson OL and Schreiber SN. *Elastic Constants and Their Measurement.* New York: McGraw-Hill Education; 1974.
31. Haines J, Leger JM and Bocquillon G. Synthesis and design of superhard materials. *Annual Review of Materials Research*. 2001; 31:1-23. http://dx.doi.org/10.1146/annurev.matsci.31.1.1
32. Pugh SF. Relation between the elastic moduli and the plastic properties of polycrystalline pure metals. *Philosophical Magazine*. 1954; 45:823-843.
33. Wachter P, Filzmoser M and Rebizant J. Electronic and elastic properties of the light actinide tellurides. *Physica B*: Condensed Matter. 2001; 293(3-4):199-223. http://dx.doi.org/10.1016/S0921-4526(00)00575-5
34. Anderson OL. A simplified method for calculating the debye temperature from elastic constants. *Journal of Physics and Chemistry of Solids*. 1963; 24(7):909-917. http://dx.doi.org/10.1016/0022-3697(63)90067-2
35. Schreiber E, Anderson OL and Soga N. *Elastic Constants and their Measurements.* New York: McGraw-Hill; 1996.